

Copyright © 2002 IEEE. Reprinted from (H.C. van Assen, M. Egmont-Petersen, J.H.C. Reiber. "Accurate object localization in gray level images using the center of gravity measure: Accuracy versus precision," *IEEE Transactions on Image Processing*, Vol. 11, No. 12, pp. 1379-1384, 2002, Copyright IEEE).

This material is posted here with permission of the IEEE. Internal or personal use of this material is permitted. However, permission to reprint/republish this material for advertising or promotional purposes or for creating new collective works for resale or redistribution must be obtained from the IEEE by writing to pubs-permissions@ieee.org.

By choosing to view this document, you agree to all provisions of the copyright laws protecting it.

For more information, see the Homepage of IEEE Transactions on Image Processing:
<http://ieeexplore.ieee.org/Xplore/DynWel.jsp>

Comments and questions can be sent to: michael@cs.uu.nl

Accurate Object Localization in Gray Level Images Using the Center of Gravity Measure: Accuracy Versus Precision

H. C. van Assen, M. Egmont-Petersen, and J. H. C. Reiber, *Senior Member, IEEE*

Abstract—A widely used subpixel precision estimate of an object center is the weighted center of gravity (COG). We derive three maximum-likelihood estimators for the variance of the two-dimensional (2-D) COG as a function of the noise in the image. We assume that the noise is additive, Gaussian distributed and independent between neighboring pixels.

Repeated experiments using 2500 generated 2-D bell-shaped markers superimposed with an increasing amount of Gaussian noise were performed, to compare the three approximations.

The error of the most exact approximative variance estimate with respect to true variance was always less than 5% of the latter. This deviation decreases with increasing signal-to-noise ratio. Our second approximation to the variance estimate performed better than the third approximation, which was originally presented by Oron *et al.* [1] by up to a factor ≈ 10 . The difference in performance between these two approximations increased with an increasing misplacement of the window in which the COG was calculated with respect to the real COG.

Index Terms—Center of gravity, centroid, measurement noise, object position, object recognition, subpixel precision, variance.

I. INTRODUCTION

OBJECT detection plays an important role in many image-processing problems. Examples from medical imaging are marker recognition [2] and leukocyte tracking. In remote sensing, tasks like automatic target recognition and delineation of particular areas entail object recognition. In such applications, it is important to determine the position of each detected object with the highest possible accuracy and precision. When the positions of the objects need to be known with subpixel precision, accurate and robust estimates can be obtained by computing their center of gravity [3].

We will present a framework for analyzing the accuracy (bias) and precision (variance) of the weighted center of gravity in the presence of noise, see Fig. 1. In this paper, we first review different noise generating processes (Section II). In Section III, the total variance is subdivided into a bias of the mean and the variance around this mean center of gravity. Subsequently, we derive a novel formula for the variance of the weighted center of gravity measure, along with two approximations. In Section IV,

Manuscript received February 13, 2001; revised June 28, 2002. The associate editor coordinating the review of this manuscript and approving it for publication was Prof. Ioannis Pitas.

The authors are with the Division of Image Processing (LKEB), Department of Radiology, Leiden University Medical Center, 2300 RC Leiden, The Netherlands (e-mail: h.c.van_assen@lumc.nl; j.h.c.reiber@lumc.nl; michael@cs.uu.nl).

Digital Object Identifier 10.1109/TIP.2002.806250

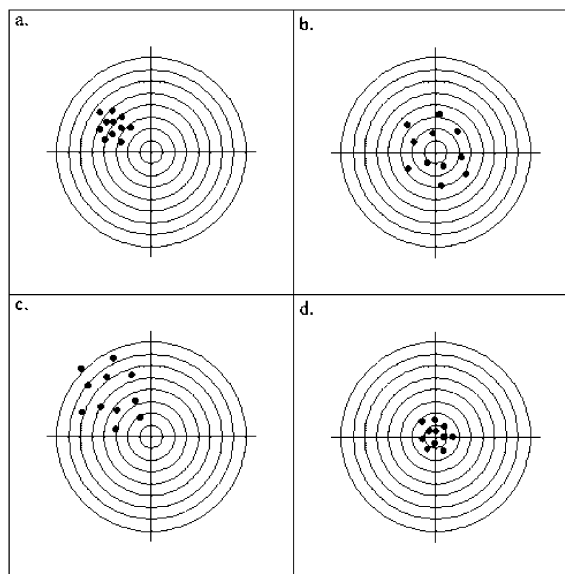


Fig. 1. (a) Estimated COG is biased, but successive realizations (in the presence of noise) show a small dispersion. (b) Estimated COG is unbiased, but highly dispersed. (c) Estimated COG is biased, and highly dispersed. (d) Optimal situation, where the estimated COG is unbiased and successive realizations show a small dispersion.

the validity of the formulas and the circumstances under which these approximations suffice are investigated experimentally. Section V contains our conclusions.

II. BACKGROUND

Define a noise-free image as a two-dimensional (2-D)¹ sampled function $F(x, y)$ of the discrete coordinates $x = 1, \dots, x_{\max}$ and $y = 1, \dots, y_{\max}$. Assume that the intensity of the pixels in a noisy image is the result of successive realizations of a random variable $\varepsilon(x, y)$. The noise-generating process is defined by the class of stochastic functions $G: \mathbb{R}^{1+d} \rightarrow \mathbb{R}$, $f(x, y) = G(F(x, y), \theta)$, with θ the d -dimensional parameter vector describing the stochastic model of G . We distinguish between three (external) general noise generating processes.

- Additive noise: $f(x, y) = F(x, y) + \varepsilon(x, y)$;
- Multiplicative noise: $f(x, y) = F(x, y) \cdot \varepsilon(x, y)$ (see, e.g., [4]);
- Impulsive (Salt-and-Pepper) noise: $f(x, y) = F(x, y) + G(F(x, y), \theta)$ (see [5]).

¹In [13] we generalize our results to 3-D-coordinates.

The simplest stochastic process is that of additive noise. In fact, the linearity of the weighted center of gravity is justified in a situation with additive noise. We limit our analysis of the weighted center of gravity to the situation with additive noise.

III. CENTER OF GRAVITY AND ITS VARIANCE

Let us define a detection function $d(x, y)$ (e.g., a filter), whose output is related to the probability that the coordinate (x, y) is the central pixel of the object to be detected. In the sequel, we assume that the value $d(x, y) \propto P(\text{center} = (x, y))$ for (x, y) being in some neighborhood, $(x, y) \in \Omega$, in the vicinity of the true object center. In a gray-level image, the weighted center of gravity of the object is defined as [3]

$$c(x, y) = \left(\frac{\sum_{x,y \in \Omega} x w(x, y)}{\sum_{x,y \in \Omega} w(x, y)}, \frac{\sum_{x,y \in \Omega} y w(x, y)}{\sum_{x,y \in \Omega} w(x, y)} \right) \quad (1)$$

with $w(x, y)$ a function that weighs the coordinates defined as $w(x, y) = a \cdot (f(x, y) - m)$ where $m < \min_{x,y \in \Omega} (f(x, y))$ when $a > 0$ or $m > \max_{x,y \in \Omega} (f(x, y))$ when $a < 0$. In the first case, where the parameter $a > 0$, the center of gravity is attracted to the brighter pixels in Ω whereas for $a < 0$, darker pixels attract $c(x, y)$. In practical applications, $m = \min_{x,y \in \Omega} (f(x, y)) - \delta$, $\delta > 0$ (e.g., 0.01) and $a = 1$ for bright-center objects, whereas $m = \max_{x,y \in \Omega} (f(x, y)) + \delta$, $\delta > 0$ and $a = -1$ for dark-center objects.

Equation (1) shows that the noise is propagated to the weighted center of gravity through the weights $w(x, y)$. Define the variance of the center of gravity for $n \rightarrow \infty$ as

$$\text{var}(c(x, y)) = n^{-1} \left(\sum_{i=1}^n (c(x) - \gamma(x))^2, \sum_{i=1}^n (c(y) - \gamma(y))^2 \right) \quad (2)$$

with $(\gamma(x), \gamma(y))$ denoting the true and $(c(x), c(y))$ the estimated center of gravity, and n the number of observations. We propose to split the variance component of the weighted center of gravity into the variance of the estimates $c(x, y)$ in relation to the estimated mean $\bar{c}(x, y)$, and the bias component, $(\bar{c}(x, y) - \gamma(x, y))^2$, which yields (see Appendix A)

$$\begin{aligned} \text{var}(c(x, y)) &= \left(n^{-1} \sum_{i=1}^n (c_x(x, y) - \bar{c}_x(x, y))^2 + (\bar{c}_x(x, y) - \gamma_x(x, y))^2, \right. \\ &\quad \left. n^{-1} \sum_{i=1}^n (c_y(x, y) - \bar{c}_y(x, y))^2 + (\bar{c}_y(x, y) - \gamma_y(x, y))^2 \right) \quad (3) \end{aligned}$$

with $\bar{c}(x, y) = (n^{-1} \sum_{i=1}^n c_x(x, y), n^{-1} \sum_{i=1}^n c_y(x, y))$. The weighted center of gravity $c(x, y)$ is only an unbiased estimator of the true center $\gamma(x, y)$ when $(\bar{c}(x, y) - \gamma(x, y))^2 \rightarrow (0, 0)$ for $n \rightarrow \infty$. In the presence of noise the variance around the mean remains (see Table II).

In order to find an expression for the variance of the quotient of two stochastic terms, (3), we start off with the delta-method²

[6], which states that for a stochastic variable Z , $\text{var}(Z) \approx \text{var}(\ln(Z)) \cdot \mu_Z^2$, where μ_Z denotes the mean of the variable Z . Let Z denote the quotient of two entities X and Y , so this approximation can be rewritten as

$$\text{var} \left(\frac{X}{Y} \right) \approx \left(\frac{\text{var}(X)}{\mu_X^2} + \frac{\text{var}(Y)}{\mu_Y^2} - 2 \cdot \frac{\text{cov}(X, Y)}{\mu_X \mu_Y} \right) \cdot \left(\frac{\mu_X}{\mu_Y} \right)^2 \quad (4)$$

with $\text{cov}(x, y)$ the covariance between X and Y . Because the centers of the x - and y -coordinates are independent, we will perform the derivation for the x -coordinate only. Define X as the numerator and Y as the denominator in (1), i.e., $X(\Omega) = \sum_{x,y \in \Omega} x w(x, y)$, and $Y(\Omega) = \sum_{x,y \in \Omega} w(x, y)$. Inserting these terms into (4) yields

$$\begin{aligned} \text{var}_x(c(x, y)) &\approx \left(\frac{\text{var} \left(\sum_{x,y \in \Omega} x w(x, y) \right)}{\mu^2 \sum_{x,y \in \Omega} x w(x, y)} + \frac{\text{var} \left(\sum_{x,y \in \Omega} w(x, y) \right)}{\mu^2 \sum_{x,y \in \Omega} w(x, y)} \right. \\ &\quad \left. - 2 \cdot \frac{\text{cov} \left(\sum_{x,y \in \Omega} x w(x, y), \sum_{x,y \in \Omega} w(x, y) \right)}{\mu \sum_{x,y \in \Omega} x w(x, y) \mu \sum_{x,y \in \Omega} w(x, y)} \right) \\ &\quad \cdot \left(\frac{\mu \sum_{x,y \in \Omega} x w(x, y)}{\mu \sum_{x,y \in \Omega} w(x, y)} \right)^2. \quad (5) \end{aligned}$$

From (1) and from the definition of $X(\Omega)$, we can estimate the mean and variance in X as $\hat{\mu}_X(\Omega) \approx N \cdot \hat{\mu}_w \cdot \hat{x}_{COG}$ and $\hat{\sigma}_X^2(\Omega) = \sigma^2 \cdot \sum_{x,y \in \Omega} x^2$, respectively, with $N = \text{card}(\Omega)$, $\hat{\mu}_w$ the estimated average of the weights in Ω , and \hat{x}_{COG} the coordinate of the estimated center of gravity, in the neighborhood Ω [7]. Similarly, the estimated average and variance of the denominator Y in (4), become $\hat{\mu}_Y = N \cdot \hat{\mu}_w$ and $\hat{\sigma}_Y^2 = N \cdot \sigma^2$, respectively. Let the center of the area Ω be the origin of the coordinate system such that the covariance term in (4) can be omitted [1]. This yields the following approximation to $\text{var}(c(x, y))$

$$\begin{aligned} \text{var}(c(x, y)) &\approx \left(\left(\frac{\sigma^2 \cdot \sum_{x,y \in \Omega} x^2}{(N \cdot \hat{\mu}_w \cdot \hat{x}_{COG})^2} + \frac{\sigma^2}{N \cdot \hat{\mu}_w^2} \right) \cdot \hat{x}_{COG}^2, \right. \\ &\quad \left. \left(\frac{\sigma^2 \cdot \sum_{x,y \in \Omega} y^2}{(N \cdot \hat{\mu}_w \cdot \hat{y}_{COG})^2} + \frac{\sigma^2}{N \cdot \hat{\mu}_w^2} \right) \cdot \hat{y}_{COG}^2 \right) \quad (6) \end{aligned}$$

with \hat{y}_{COG} the estimated center of gravity in the y -direction. If the object is positioned centrally inside the neighborhood Ω of the marker's center of gravity (i.e., \hat{x}_{COG} and \hat{y}_{COG} are very close to zero) the second terms inside the brackets in (6) (i.e.,

²In [13] we specify the conditions under which this approximation holds.

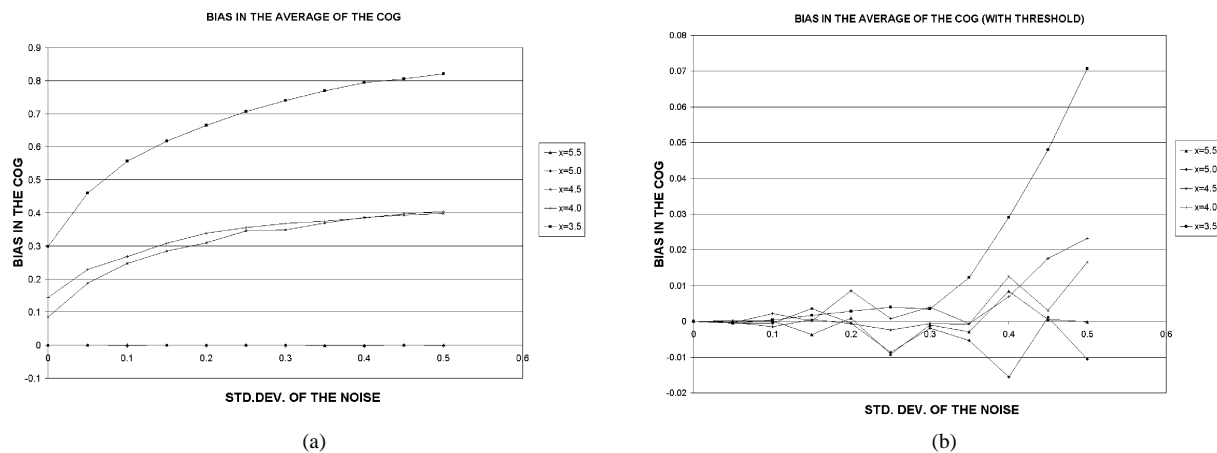


Fig. 2. Bias in the mean of the COG (for the x -coordinate) of a marker as a function of the standard deviation of the noise in the gray levels. The different series indicate different window misplacements ($x = 5.5$ means that the window was placed centrally on the marker). (a) Without application of a threshold. (b) With application of a threshold.

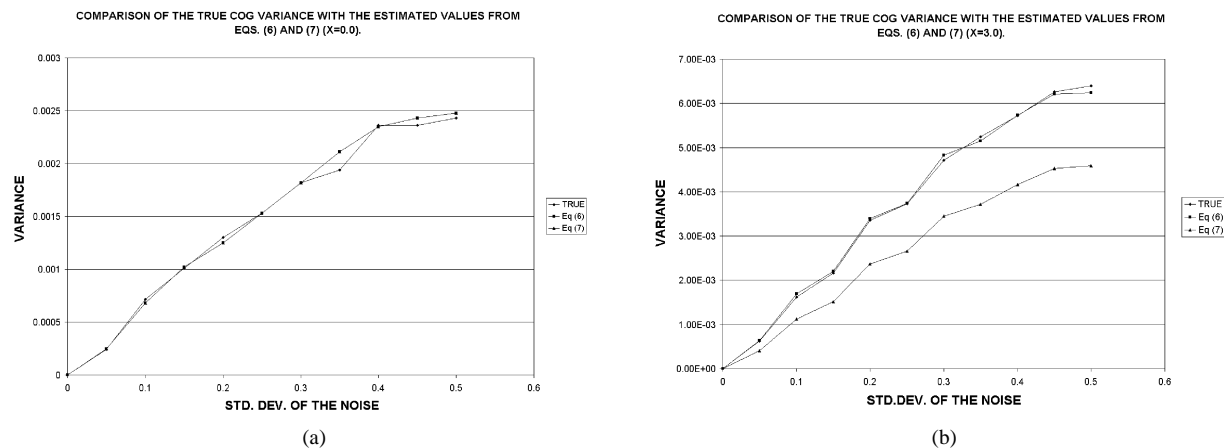


Fig. 3. Comparison of the true variance of the COG from simulation data with values from equations (6) and (7). The origin of the coordinate system was placed at the COG. (a) Window was placed centrally on the marker. (b) Window was misplaced along the x -direction by 3.0 pixels.

$\sigma^2/N \cdot \hat{\mu}_w^2$) can also be neglected and, thus, (5) simplifies to the approximation derived by Oron *et al.* [1]

$$\text{var}(c(x, y)) \approx \left(\frac{\sigma^2 \cdot \sum_{x,y \in \Omega} x^2}{(N \cdot \hat{\mu}_w)^2}, \frac{\sigma^2 \cdot \sum_{x,y \in \Omega} y^2}{(N \cdot \hat{\mu}_w)^2} \right). \quad (7)$$

IV. EXPERIMENTS

A. Experimental Setup

Simulations with synthetic objects were carried out to investigate the accuracy of the derived variance estimators (5)–(7). We conducted a number of simulations in which 2500 markers with a (2-D) circular bell shape [8] and a size of 10×10 pixels were generated. The gray values of the centers of the markers were set close to 2 whereas the values at the edges were close to 0. Gaussian zero-centered noise with $\sigma = 0.0, \dots, 0.5$ with steps of 0.05 was superimposed on the markers. Two experiments were performed using a 10×10 neighborhood Ω . Additionally, one experiment was performed to measure image deformation.

B. Experiment 1—Misplacing the Window

We investigated the influence of translating the object away from the center of the window [having coordinates (5.5, 5.5)] along the x -axis. Fig. 2(a) shows the results from the first experiment. Fig. 2(b) shows that applying a threshold to the marker images before calculating the centers of gravity reduces the intrinsic bias toward the center of Ω . The threshold was applied such that the center of gravity was always based on the 16 largest gray values in the window Ω . It is clear from this experiment that the bias caused by misplacing the window can be reduced by application of a threshold.

C. Experiment 2 Precision of the Approximate Variance Estimators

In the second experiment, the true variance of the center of gravity estimates was compared to the approximations from (6) and (7). The variances were compared, for markers translated by 0, 1.5 (not shown) and 3.0 pixels along the x -direction.

The simulations show that (6) is a good approximation to the true resulting variance of the center of gravity measure [Fig. 3(a) and (b)], and (7) is a good approximation if the marker is positioned centrally in the window. From this experiment, it is clear that (6) outperforms (7), the approximation derived by Oron *et*

TABLE I

RESULTS OF TWO-SIDED STUDENT'S T -TEST WITH HYPOTHESIS H_0 : TWO HORIZONTAL OR VERTICAL DISTANCES ARE EQUAL. THE CRITICAL VALUE FOR T WAS 2.101, WITH $1 - \alpha = 0.975$ AND $\nu = 18$. IN THE TABLE, d_1 IS THE UPPERMOST, d_2 THE MIDDLE AND d_3 THE LOWEST HORIZONTAL DISTANCE AND d_4 IS THE LEFTMOST, d_5 THE MIDDLE AND d_6 THE RIGHTMOST VERTICAL DISTANCE. WITH DECREASING SNR, THE HYPOTHESIS H_0 CAN BE REJECTED IN A DECREASING NUMBER OF TESTS

Horizontal distances ($\alpha = 0.05$)						
H_0	SNR=24.3 dB		SNR=18.3 dB		SNR=12.3 dB	
	T-value	Reject H_0 ?	T-value	Reject H_0 ?	T-value	Reject H_0 ?
$d_1 = d_2$	-3.53	Yes	-1.82	No	-1.03	No
$d_2 = d_3$	3.83	Yes	2.17	Yes	1.24	No
$d_1 = d_3$	0.51	No	0.47	No	0.29	No
Vertical distances ($\alpha = 0.05$)						
H_0	SNR=24.3 dB		SNR=18.3 dB		SNR=12.3 dB	
	T-value	Reject H_0 ?	T-value	Reject H_0 ?	T-value	Reject H_0 ?
$d_4 = d_5$	-3.59	Yes	-2.21	Yes	-0.94	No
$d_5 = d_6$	0.43	No	0.27	No	-0.51	No
$d_4 = d_6$	-3.02	Yes	-1.85	No	-1.31	No

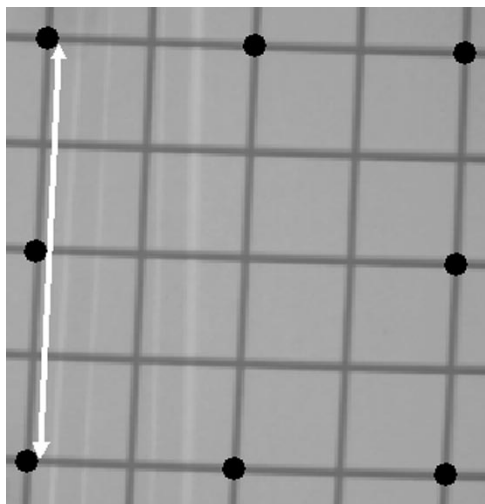


Fig. 4. Radiograph of the rectangular grid used in experiment three. The band crossings used to measure the horizontal and vertical distances are indicated with black dots. All the distances measured were distances over 4 cells (white arrow illustrates the cord).

al. [1], when Ω is not centered on the center of gravity of the marker.

D. Experiment 3—Assessment of Image Deformation

In this experiment, we used a radiograph of a rectangular calibration grid [Fig. 4(a)] to assess the amount of image deformation caused by pincushion distortion. An image of the grid was acquired with a tube voltage of 60 kV and convolved with the LoG (Laplacian of the Gaussian kernel) [9] in order to find the crossings of the horizontal and vertical bands. The crossings' locations were roughly estimated using the Hough Transform [10]. Before

calculating each center of gravity from the radiograph itself, the neighborhood Ω was superimposed with additive Gaussian noise with a specific variance. Table I shows the results of the Student's T -tests for the hypothesis H_0 : two parallel cords have the same length. It appears from Table I that when the SNR deteriorates, the number of significantly different cord lengths, for which the hypothesis H_0 can be rejected, decreases.

V. DISCUSSION

Both the estimated center of gravity and its variance depend on the size of the window that encompasses the pixels that are regarded as belonging to the object. It is clear from both (6) and (7) that a larger N leads to a decrease in the variance as N occurs in the denominators of both variance formulas. Decreasing the size of the window, on the other hand, diminishes the probability that pixels that do not belong to the particular object enter the calculation. Hence, the center of gravity may be estimated more accurately, because this decreases the averaging bias (see Table II).

Our simulations indicate that a threshold should in general be applied. Several automatic methods have been developed for optimal threshold selection, for a discussion, see, e.g., [11]. Which threshold value is optimal for estimating the center of gravity, depends on the intensity pattern surrounding the object center, the chosen window size, the level of the noise present and the preferred tradeoff between the (inversely related) averaging bias and discretization bias, and variance. A high threshold implies that only a few pixels enter the computation. A low threshold results in more averaging, because more pixels enter the center-of-gravity calculation, such that noise has less influence on the center of gravity estimate. However, this compromises the accuracy (averaging bias) in the sense that the center of gravity estimate becomes biased by the positioning of the window (see Table II).

TABLE II

THIS TABLE SUMMARIZES THE RESULTS FOUND IN OUR SIMULATION STUDIES. THE UP-ARROW IN CELL (1,1), WHICH COMBINES BIAS WITH INCREASING WINDOW SIZE, INDICATES THAT INCREASING THE WINDOW SIZE WILL INCREASE THE BIAS IN THE CENTER OF GRAVITY ESTIMATE COMPARED WITH THE TRUE OBJECT CENTER. THE DOWN-ARROW IN CELL (2,1), WHICH COMBINES VARIANCE WITH INCREASING WINDOW SIZE, INDICATES THAT INCREASING THE WINDOW SIZE WILL DECREASE THE VARIANCE IN THE ESTIMATED CENTER OF GRAVITY. A 0, E.G., IN CELL (5,1), INDICATES THAT SHIFTING THE OBJECT HAS NO EFFECT ON THE BIAS WHEN A THRESHOLD IS APPLIED BEFORE THE COG IS COMPUTED

Factor	Increasing window size	Thresholding	Poorer signal-to-noise ratio	Shifting object (no threshold)	Shifting object (with threshold)
Bias	↑	↓*↑**	↑***	↑	≈0
Variance	↓	↑	↑	↑	≈0

* Increasing the threshold leads to a smaller averaging bias

** Increasing the threshold leads to a larger discretization bias

*** Poorer SNR may result in more averaging bias, due to random peaks that enter the COG-computation

VI. CONCLUSION

In this paper, we have studied the behavior of the (weighted) center of gravity estimate as a function of additive noise present in gray value images. Furthermore, we analyzed the influence of applying a threshold to the gray value image (which determines the weighing scheme) for a possible bias and variance of the center of gravity measure. The decision whether to apply a threshold to the gray value image or not, is basically a choice between accuracy and precision. Application of a threshold before the center of gravity is computed, results in general in a better accuracy (smaller bias) but a worse precision. For a specific application where the exact object centers should be known, we recommend experiments be conducted to establish the desired tradeoff between bias and variance. Our variance formula makes it possible to estimate the tradeoff between accuracy and precision, in the presence of noise. Factors that can be varied are listed in Table II. We have compared three formulas for the estimation of the variance of the center of gravity measure with the true variance. Our approximation (6) performs much better than the one presented by Oron [1] (7), when the evaluation window Ω is not centered on the true center of gravity. Because the true center of gravity is generally unknown beforehand, a misplacement of the window Ω might easily occur. In this case, if an estimation of the precision of the center of gravity measure is requested, our novel estimator (6) should be applied. In conclusion, we can state that in order to find the best estimate for the center of gravity in a gray level image, a threshold should in general be applied to (the local neighborhood in) the image before calculating a center of gravity measure.

APPENDIX

In Section IV, we define the variance of the center of gravity for $n \rightarrow \infty$ as

$$\text{var}(c(x, y)) = n^{-1} \left(\sum_{i=1}^n (c_x(x, y) - \gamma_x(x, y))^2, \sum_{i=1}^n (c_y(x, y) - \gamma_y(x, y))^2 \right) \quad (\text{A.1})$$

with $(\gamma_x(x, y), \gamma_y(x, y))$ denoting the true and $(c_x(x, y), c_y(x, y))$ the estimated center of gravity and n the number of observations. Next, we propose to divide the variance component of the weighted center of gravity into the variance of the estimates $c(x, y)$ in relation to the estimated mean $\bar{c}(x, y)$ and the (squared) bias component [7], [12], $(\bar{c}(x, y) - \gamma(x, y))^2$.

In order to achieve this, we subtract and add (only x -components are shown, y -components are identical) $\bar{c}_x(x, y)$ to the term $(c_x(x, y) - \gamma_x(x, y))^2$ in (A.1). This yields

$$\text{var}_x(c(x, y)) = n^{-1} \sum_{i=1}^n ((c_x(x, y) - \bar{c}_x(x, y)) + \bar{c}_x(x, y) - \gamma_x(x, y))^2. \quad (\text{A.2})$$

Expanding the quadratic term, gives us

$$\begin{aligned} \text{var}_x(c(x, y)) &= n^{-1} \sum_{i=1}^n (c_x(x, y) - \bar{c}_x(x, y))^2 \\ &\quad + n^{-1} \sum_{i=1}^n (\bar{c}_x(x, y) - \gamma_x(x, y))^2 \\ &\quad + 2n^{-1} \sum_{i=1}^n (c_x(x, y) - \bar{c}_x(x, y)) \\ &\quad \quad \cdot (\bar{c}_x(x, y) - \gamma_x(x, y)). \quad (\text{A.3}) \end{aligned}$$

In (A.3), the term $(\bar{c}_x(x, y) - \gamma_x(x, y))$ is a constant and because of the definition of $\bar{c}(x, y)$ in (7) the term $n^{-1} \sum_{i=1}^n (c_x(x, y) - \bar{c}_x(x, y))$ is equal to zero. Substituting this finding in (A.3), results in

$$\text{var}_x(c(x, y)) = n^{-1} \sum_{i=1}^n (c_x(x, y) - \bar{c}_x(x, y))^2 + n^{-1} \sum_{i=1}^n (\bar{c}_x(x, y) - \gamma_x(x, y))^2 \quad (\text{A.4})$$

which is equal to the x -component of (6).

REFERENCES

- [1] E. Oron, A. Kumar, and Y. Bar-Shalom, "Precision tracking with segmentation for imaging sensors," *IEEE Trans. Aerosp. Electron. Syst.*, vol. 29, no. 3, pp. 977–987, 1993.
- [2] H. C. Van Assen, H. A. Vrooman, M. Egmont-Petersen, J. G. Bosch, G. Koning, E. L. Van Der Linden, B. Goedhart, and J. H. C. Reiber, "Automated calibration in vascular X-ray images using the accurate localization of catheter marker bands," *Invest. Radiol.*, vol. 35, no. 4, pp. 219–226, 2000.
- [3] R. C. Gonzalez and R. E. Woods, *Digital Image Processing*. Reading, MA: Addison-Wesley, 1992.
- [4] B. Aiazzi, L. Alparone, and S. Baronti, "Multiresolution local-statistics speckle filtering based on a ratio Laplacian pyramid," *IEEE Trans. Geosci. Remote Sensing*, vol. 36, no. 5, pp. 1466–1476, 1998.
- [5] E. M. Eliason and A. S. McEwan, "Adaptive box filters for removal of random noise from digital images," *Photogramm. Eng. Remote Sens.*, vol. 56, no. 4, pp. 453–458, 1990.
- [6] C. Cox, "Delta method," in *Encyclopedia of Biostatistics*, P. Armitage and T. Colton, Eds. Chichester, U.K.: Wiley, 1998, pp. 1125–1127.
- [7] M. B. Priestley, *Spectral Analysis and Time Series*, 7th ed. London, U.K.: Academic, 1992, p. 890.
- [8] M. Egmont-Petersen and T. Arts, "Recognition of radiopaque markers in X-ray images using a neural network as nonlinear filter," *Pattern Recognit. Lett.*, vol. 20, no. 5, pp. 521–533, 1999.
- [9] B. M. Dawant and A. P. Zijdenbos, "Image segmentation," in *Medical Imaging*, M. Sonka and J. M. Fitzpatrick, Eds. Bellingham, WA: SPIE, 2000, pp. 71–127.
- [10] P. V. C. Hough, "A method and means for recognizing complex patterns," U.S. Patent, 1962.
- [11] J.-S. Chang, H.-Y. M. Liao, M.-K. Hor, J.-W. Hsieh, and M.-Y. Chern, "New automatic multi-level thresholding technique for segmentation of thermal images," *Image Vis. Comp.*, vol. 15, pp. 23–34, 1997.
- [12] M. P. Wand and M. C. Jones, *Kernel Smoothing*. London, U.K.: Chapman & Hall, 1995.
- [13] H. C. Van Assen, M. Egmont-Petersen, and J. H. C. Reiber. (2001) Accurate object localization in gray level images using the center of gravity measure; accuracy versus precision. [Online]. Available: <http://www.cs.uu.nl/pub/RUU/CS/techreps/CS-2001/2001-57.pdf>. Tech. Rep. UU-CS-2001-57

H. C. van Assen was born in Leeuwarden, The Netherlands, in 1969. He received his M.Sc. degree in applied physics from the Delft University of Technology in 1995.

He has been working for the Laboratory for Clinical and Experimental Image Processing (LKEB) at the Leiden University Medical Center since 1996. His research interests include quantitative vascular angiography (QVA) and knowledge guided model based 3-D image segmentation. His current research involves knowledge driven automated segmentation in temporal and spatial cardiovascular image sequences which will be the basis for his Ph.D. thesis.

Mr. van Assen is a member of the Dutch society for Pattern Recognition and Image Processing.

M. Egmont-Petersen was born in Copenhagen, Denmark, in 1967. He received the combined B.Sc. and combined M.Sc. degrees in computer science/business administration from Copenhagen Business School in 1988 and 1990, respectively. He received the Ph.D. degree in medical informatics from Maastricht University, Maastricht, The Netherlands, in 1996.

He currently works for the Institute of Computer and Information Sciences, Utrecht University, Utrecht, The Netherlands, as a Postdoctoral Researcher. His current research focuses on probabilistic networks, statistical pattern recognition and knowledge-based image interpretation. He has published more than 60 papers in scientific journals, books, and conference proceedings.

Dr. Egmont-Petersen is a member of the IEEE Computer Society, the Dutch society for Pattern Recognition and Image Processing, and working group TC9 (Biomedical Pattern Recognition) under the auspices of ICPR.

J. H. C. Reiber (M'75–SM'84) was born in Haarlem, the Netherlands, in 1946. He received the M.Sc.E.E. degree from the Delft University of Technology in 1971 and the Ph.D. degree in electrical engineering in 1976 from Stanford University, Stanford, CA.

In 1977, he founded the Laboratory for Clinical and Experimental Image Processing (LKEB) at the Thoraxcenter in Rotterdam, directing the research at the development and validation of objective and automated techniques for the segmentation of cardiovascular images, in particular for quantitative coronary arteriography (QCA), nuclear cardiology and echocardiography. With the move of LKEB in 1990 to the Leiden University Medical Centre (LUMC), the scope broadened to intravascular ultrasound, MRI, MSCT, etc., also in radiological applications. Since April 1995 he has been a Professor of Medical Image processing, in particular in cardiovascular applications at the LUMC and the Interuniversity Cardiology Institute of the Netherlands (ICIN). His research interests include (knowledge guided) image processing and its clinical applications.

Dr. Reiber is a member of the Royal Netherlands Academy of Arts and Sciences.